



Novel Self-Assembled Morphologies from Isotropic Interactions

E. Edlund, O. Lindgren, and M. Nilsson Jacobi*

Complex Systems Group, Department of Energy and Environment, Chalmers University of Technology, SE-41296 Göteborg, Sweden
(Received 20 April 2011; revised manuscript received 22 June 2011; published 15 August 2011)

We present results from particle simulations with isotropic medium range interactions in two dimensions. At low temperature novel types of aggregated structures appear. We show that these structures can be explained by spontaneous symmetry breaking in analytic solutions to an adaptation of the spherical spin model. We predict the critical particle number where the symmetry breaking occurs and show that the resulting phase diagram agrees well with results from particle simulations.

DOI: 10.1103/PhysRevLett.107.085501

PACS numbers: 81.16.Dn, 05.65.+b, 75.10.Hk, 89.75.Kd

Understanding the principles behind the spontaneous formation of structured morphologies is of interest both as a fundamental scientific question and in engineering applications where the possibility of using self-assembly to produce novel materials provides a compelling complement to traditional blueprinted fabrication [1,2]. Consequently there is growing interest in exploring interactions that can facilitate self-fabrication of materials with novel properties [3–5]. The more general question of what structures are possible to self-assemble from a given class of interactions has however not been addressed, with some notable exceptions, e.g., simulation-based analysis of polyhedral packing [6].

To examine the possibilities of self-assembly from a theoretical angle, in this Letter we consider systems with pairwise isotropic interactions, frequently used as coarse-grained models of more complex mesoscale systems such as colloidal systems [7], particles in an ambient fluid [8], and spin glasses [9]. We show that typical aggregates appearing as low-temperature configurations in particle simulations with randomly generated medium range isotropic interactions can be predicted analytically using an adaptation of the spherical spin model [10]. The morphologies, many of them novel and surprisingly complex, can be systematically classified by their spontaneous breaking of the rotational symmetry.

To formulate a solvable model of a particle system we start by considering a lattice spin system with Hamiltonian of the form

$$H = \sum_{ij} U_{ij} s_i s_j, \quad (1)$$

where $s_i \in \{0, 1\}$, and $s_i = 1$ represents a particle at lattice site i and $s_i = 0$ represents vacuum. The total number of particles is set by the normalization $\sum_i s_i = N$. The interaction U_{ij} is an effective isotropic potential with a hard core repulsion corresponding to the lattice spacing. In a spin glass metal the interaction is mediated by a polarization of the Fermi sea [11] while in a colloidal system it could involve a surface polymer induced steric hindrance competing with a depletion attraction [12].

The discrete model described by Eq. (1) can equivalently be formulated as a continuous one ($s_i \in \mathbb{R}$) with auxiliary constraints, $\sum_i s_i^m = N \forall m$. To make the model analytically tractable we relax the constraints to include only the first two moments. The result is the spherical spin model with an external field, with Hamiltonian $H_s = \sum_{ij} U_{ij} s_i s_j + h \sum_i s_i$. In general there is no guarantee that this approximation will produce relevant results, but as we will see, typically there is a strong correspondence between the discrete and continuous models. The main idea in this study is that the ground states in the continuous model can be derived analytically and that these can be used to predict the low-temperature morphologies of the discrete particle systems.

A necessary condition for an energy minimum in the spherical model is $\sum_j (U_{ij} - \lambda \delta_{ij}) s_j = h/2$, where δ is the identity matrix, and λ comes from the constraint on the second moment. Translational invariance implies that $s_i = c$ is a solution. Nonconstant solutions $s_i = v_i + c$ exist if λ is an eigenvalue of the matrix U corresponding to the eigenvector v . From the constraints it follows that $c = \rho$, where ρ is the density, and $V^{-1} \sum_i v_i^2 = (1 - \rho)\rho$, where V is the number of lattice sites or the volume. The ground states are defined by the eigenvector(s) corresponding to the lowest eigenvalue of U .

It can be shown, e.g., using translational invariance, that all isotropic interaction matrices have the Fourier modes as eigenvectors. This also follows from the observation that any such matrix U_{ij} can be expressed as a linear combination of matrices of the form $\Delta_+^l \Delta_\times^m$, $l, m = 0, 1, \dots$, where the two components are the discrete Laplace operator defined as usual Δ_+ or along the diagonals Δ_\times (note that Δ_+ and Δ_\times commute). The Fourier modes are eigenfunctions of the Laplace operator so the two arguments lead to the same conclusion. However, the latter argument points to a subtlety: the eigenfunctions of the Laplacian depend on the boundary conditions, where the Fourier harmonics result from periodic boundaries. Requiring that the functions converge to zero at infinity instead results in cylindrical harmonic eigenfunctions with angular modulations localized around a nucleation point. These localized

configurations bear similarity to topological defects, such as the Belavin-Polyakov monopole, that are important for the low-temperature behavior of, e.g., Heisenberg ferromagnets [13].

Our central result is that, when there are too few particles to occupy a translational invariant ground state, the eigenfunctions of Bessel type $J_\omega(2\pi kr)\cos(\omega\theta)$ determine the low-temperature behavior of self-assembling particle systems in two dimensions. The eigenvalues, i.e., the energies, are given by the radial Fourier transform of the potential as [14,15]

$$E(k) = 2\pi \int_0^\infty r dr U(r) J_0(2\pi kr), \quad (2)$$

so that the wave number $\kappa = \text{argmin}_k E(k)$ defines an eigenfunction with minimal energy. The energy spectrum is degenerate since $E(k)$ is independent of ω , reflecting the rotational invariance around the nucleation point. However, this degeneracy is broken by the nonlinearity in the mapping from the spherical model H_s to the discrete lattice system (1), where a single base frequency ω together with its overtones (similar to the harmonic overtones of a square wave) are energetically favored. The spontaneous symmetry breaking of the ground state, from $O(2)$ to one of its isotropy subgroups D_ω , is equivalent to the behavior in a bifurcation problem [16,17]. The ground states of the spherical model of relevance to the self-assembly problem in (1) are therefore of the form

$$\sum_{n=0}^{\infty} a_n J_{n\omega}(2\pi\kappa r) \cos(n\omega\theta) + c J_0(2\pi\kappa r) \quad (3)$$

in the limit $k_m \rightarrow 0$, which turns the last term (which we refer to as the mass builder) into the translational invariant constant c in the minimization of H_s . However, the $k_m \rightarrow 0$ limit is only relevant for infinite structures (with nonzero global density). For an aggregated structure with finite mass a small but nonzero k_m is needed to localize the

solution (resulting in a nonzero local density but a global density of zero).

As we will see later, the sum in Eq. (3) is dominated by the first few terms and in practice most structures are adequately described by the zeroth and first term. Notable exceptions are finite lattices, see, e.g., Fig. 1(e), which grow by successively including higher terms.

To connect the above results to the particle model (1), we map the continuous ground states ($s_i \in \mathbb{R}$) to particle configurations ($s_i \in \{0, 1\}$) by applying a step function threshold. The energy of the resulting discrete configurations depends on how the mapping distorts the power spectrum relative to the energy spectrum (2). While the main weight of the discrete configurations typically remains localized to κ , contributions from overtones that appear in the discrete system can have a large effect on the energy. These effects are difficult to quantify analytically. Instead we generate possible candidates for ground states using Eq. (3), i.e., linear combinations of Bessel functions with angular frequencies $0, \omega, 2\omega$, and 3ω with $\kappa = 1$, as well as a mass-building Bessel function with $\omega = 0$ and k_m chosen such that the first zero of J_ω for $\sigma = 1, 2, 3$. The configurations were mapped to binary valued configurations on a lattice with a threshold that defines different masses. The energy of the resulting configurations was calculated for 1000 random first-order spline potentials. We used aggregating potentials, i.e., potentials with a global minimum in the energy spectrum at $k = 0$. In addition, their arguments were scaled so that the interior minimum in the energy spectrum resided at $\kappa = 1$ as demonstrated in Fig. 2(a) and were attractive at the lattice distance to ensure correct resolution of the lattice. For each potential and mass we recorded the configuration with the lowest energy, which resulted in a limited number of favored morphologies, shown in Fig. 1.

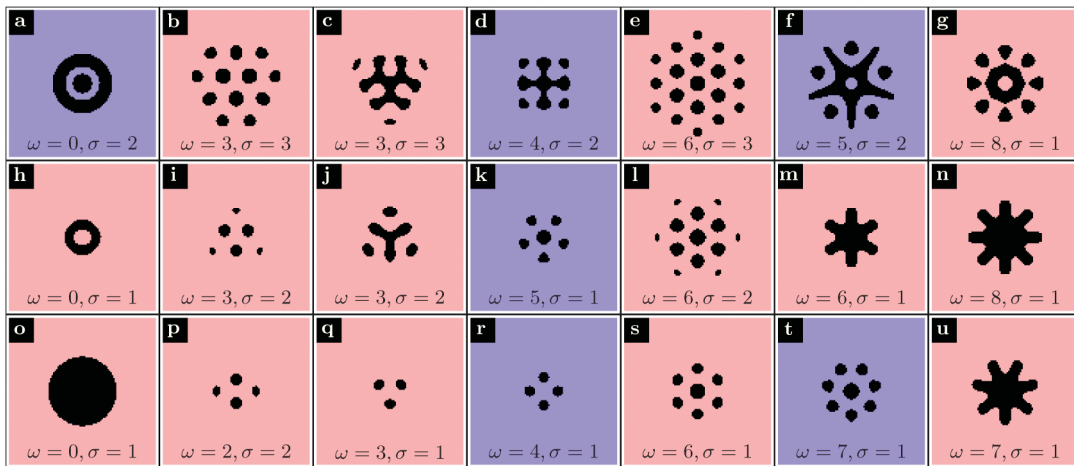


FIG. 1 (color). Predicted morphological alphabet for aggregating potentials generated by Eq. (3) (with $\omega \leq 8$). The morphologies shown are energetically preferable for a large fraction of random potentials. Red background indicates a strong signal while blue background signifies weaker signal. σ denotes the number of active radial oscillations of the ground frequency after the threshold mapping.

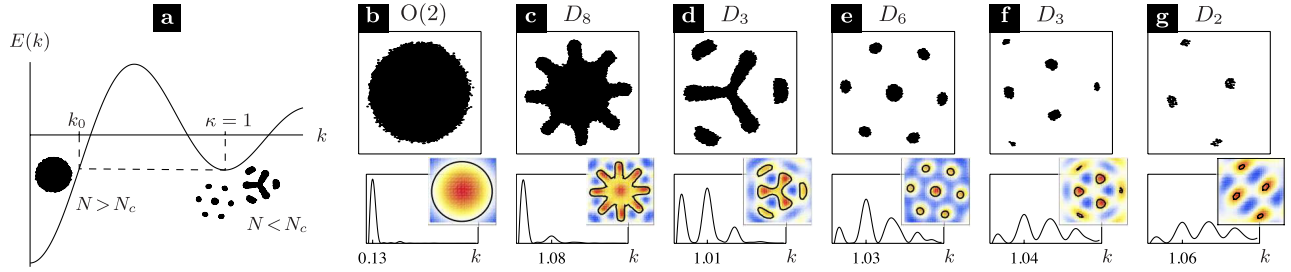


FIG. 2 (color online). Self-assembled morphologies for a single potential. (a) A typical energy spectrum of a random potential. The wavelength of the morphologies is determined by the interior minimum κ of the spectrum when the number of particles N is less than N_c , the number required to build a disk with radius corresponding to k_0 ; see Eq. (4). (b)–(g) Transitions between different symmetry groups for the potential of (a) as the particle number is decreased. (Top) Configurations from annealed particle simulations, (middle) corresponding states of the spherical model with contours added at a level giving correct number of particles, and (bottom) Bessel spectra (arb. units) of the particle configurations expanded on the form of (3), summed over ω . The first maximum corresponds to the mass builder k_m , the second should be compared to $\kappa = 1$ predicted from the spectrum in (a), and the rest are overtones.

The method predicts many novel structures [e.g., Figs. 1(a), 1(c), 1(d), 1(g), 1(h), and 1(m)], as well as simpler ones like disks and localized lattices [e.g., Figs. 1(b), 1(e), 1(l), and 1(q)]. The latter are observed on the atomic scale [18], while the former morphologies are only expected to appear at higher particle numbers.

To summarize the predictions of the adapted spherical spin model, we expect a particle system with an aggregating potential to show (I) morphologies from a limited alphabet (Fig. 1) with (II) a single dominant (base) wavelength κ determined by the minimum of the spectrum and (III) an ω degeneracy where a single potential can self-assemble into many different morphologies, depending on external parameters.

To test these predictions we performed off-lattice simulations of particle systems. We constructed 1200 random interaction potentials (piecewise constant and 3rd order splines with the same restrictions on the spectrum as above) and did Monte Carlo annealing at different particle numbers. Examples of the resulting particle configurations are shown in Figs. 2 and 3 and are in good agreement with (I). Of the simulated particle systems, approximately 86% [Fig. 3(a)] annealed to predicted morphologies shown in Fig. 1 and 9% [Fig. 3(c)] to morphologies described by Eq. (3) but absent in Fig. 1 due to the limited parameter range considered (e.g., $\omega \leq 8$). The latter were in general similar to those in Fig. 1. The strengths of the signals of the predicted morphologies in Fig. 1 were also consistent with how frequent the corresponding configurations were observed in simulations. The remaining 5% of the morphologies exhibited hierarchies of Bessel-like structures; for an example, see Fig. 3(b).

By expressing the observed particle configurations in the Bessel basis we confirm that (II) the dominant wave number is accurately predicted by the minimum in the energy spectrum of the potential. Examples of this are shown in Figs. 2(b)–2(g), where we note that while the point symmetry of the preferred configuration for a single potential

changes with varying particle number, the dominant (non-mass-building) active wavelength is approximately constant and equal to the predicted value κ . This switching of symmetry group is observed frequently in the simulations and shows that (III) the ω degeneracy is not just a mathematical curiosity in our model. For a given potential the particle number sets the morphology, an important fact that could facilitate the use of standard techniques such as density gradient centrifugation [19] for differential selection of morphologies [20].

The spectral analysis also allows us to analytically predict a phase diagram for aggregating potentials. The spectrum shown in Fig. 2(a) is typical for the potentials we consider in that it is oscillatory and has a global minimum at $k = 0$. In a spin system a global minimum at $k = 0$

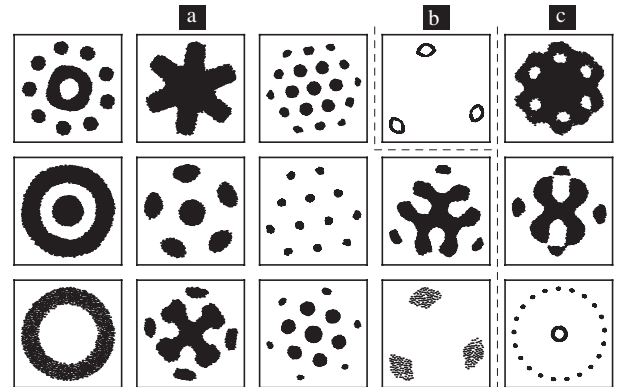


FIG. 3. Examples of configurations from particle simulations with randomly generated potentials. All configurations except (b) are well represented by functions on the form (3) with the first four terms included, most requiring only one or two. (a) Morphologies predicted as common by our method; see Fig. 1. (b) An example of a hierarchical structure, not directly describable in our theory, where each part of the usual Bessel structure serves as the nucleation point for a separate Bessel structure. (c) Morphologies that, while being simply representable by Eq. (3), are not predicted in Fig. 1.

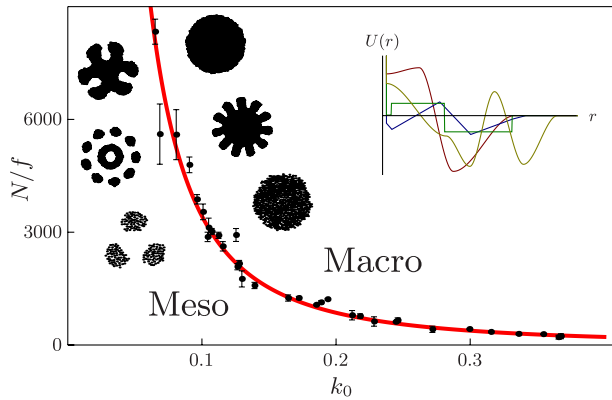


FIG. 4 (color online). Decreasing the number of particles causes a transition from disklike structures at the macroscale to more complex morphologies at the mesoscale. The figure shows the phase diagram with the predicted (full line) and measured (markers) critical number of particles N_c , adjusted for packing fraction f versus k_0 calculated [see Fig. 2(a)] from respective spectra for 33 random potentials. Inset: Four examples of potentials used.

implies a ferromagnetic ground state. For a particle system it implies that in the high particle limit we can use large scale interface minimization to argue that the ground state is dominated by the mass builder, typically a closely packed disk with a surface that is smooth or has wavelike indentations [similar to Fig. 2(c)]. For a given number of particles there is a maximal size of such a disk and for low particle numbers this effectively excludes the small k part of the energy spectrum in the minimization that determines κ . This causes a transition as the particle number is decreased, from a disk to the more complex Bessel-based morphologies we observe. This transition happens when the energy of the disk rises above the energy of the lowest interior minimum $E(\kappa)$. We denote this point k_0 , as illustrated in Fig. 2(a). The critical particle number N_c can be predicted through

$$N_c = \frac{f}{a^2} \frac{b^2}{k_0^2}, \quad (4)$$

where f is the packing fraction, a is the radius of the particles, and $b \approx 0.293$ is a numerical constant corresponding to the optimal k to describe a disk of radius 1, found through $\operatorname{argmax}_k \int_0^1 J_0(2\pi kr) r dr / \|J_0(k)\|$. The phase diagram predicted by Eq. (4) is shown in Fig. 4 together with simulation results.

Note that though the results presented in this Letter are limited to two dimensions, the analytic solution of the spherical model is the same in higher dimensions with the Bessel harmonics being replaced with spherical harmonics. Whether the connection to the particle systems remains equally clear is a question for future work, though our preliminary investigations suggest this being the case.

We conclude that isotropic pairwise additive potentials can give rise to complex morphologies appearing between

the atomic and macroscopic scale and that the frequently occurring structures form a limited morphological alphabet. The patterns are generically constructed as discretized linear combinations of a few Bessel functions, which can be understood and analytically predicted from an adaptation of the spherical spin model. Further, we analytically calculate the phase diagram showing where these patterns occur for different potentials. The accuracy of the predictions is surprising considering the complexity involved in determining the ground states in a many particle system. The methodology we present applies to the entire class of isotropic interaction potentials and provides new theoretical understanding of self-assembly processes.

O. L. and M. N. J. acknowledge support from the SuMo Biomaterials center. We thank Kolbjørn Tunstrøm for valuable comments and discussions.

*mjacobi@chalmers.se

- [1] J. Lehn, *Science* **295**, 2400 (2002).
- [2] S. Zhang, *Nat. Biotechnol.* **21**, 1171 (2003).
- [3] M. C. Rechtsman, F. H. Stillinger, and S. Torquato, *Phys. Rev. Lett.* **95**, 228301 (2005).
- [4] Q. Chen, S. C. Bae, and S. Granick, *Nature (London)* **469**, 381 (2011).
- [5] M. C. O'Sullivan, J. K. Sprafke, D. V. Kondratuk, C. Rinfray, T. D. W. Claridge, A. Saywell, M. O. Blunt, J. N. O'Shea, P. H. Beton, M. Malfois, and H. L. Anderson, *Nature (London)* **469**, 72 (2011).
- [6] U. Agarwal and F. A. Escobedo, *Nature Mater.* **10**, 230 (2011).
- [7] F. Oosawa and S. Asakura, *J. Chem. Phys.* **22**, 1255 (1954); S. Asakura and F. Oosawa, *J. Polym. Sci.* **33**, 183 (1958); A. Vrij, *Pure Appl. Chem.* **48**, 471 (1976).
- [8] F. Ercolessi and J. B. Adams, *Europhys. Lett.* **26**, 583 (1994); A. P. Lyubartsev and A. Laaksonen, *Phys. Rev. E* **52**, 3730 (1995).
- [9] M. W. Klein and R. Brout, *Phys. Rev.* **132**, 2412 (1963).
- [10] R. J. Baxter, *Exactly Solved Models in Statistical Mechanics* (Academic, London, 1982).
- [11] K. H. Fischer and J. A. Hertz, *Spin Glasses* (Cambridge University Press, Cambridge, England, 1993).
- [12] C. Likos, *Phys. Rep.* **348**, 267 (2001).
- [13] A. Belavin and A. Polyakov, *JETP Lett.* **22**, 245 (1975).
- [14] E. Edlund and M. N. Jacobi, *Phys. Rev. Lett.* **105**, 137203 (2010).
- [15] The eigenvalues are independent of the eigenbasis and (2) is from [14], where the Bessel function in the integral has no direct relation to the Bessel eigenfunctions of the Laplacian.
- [16] P. C. Matthews, *Phys. Rev. E* **67**, 036206 (2003).
- [17] R. Hoyle, *Pattern Formation* (Cambridge University Press, Cambridge, England, 2006).
- [18] H. Häkkinen, B. Yoon, U. Landman, X. Li, H. Zhai, and L. Wang, *J. Phys. Chem. A* **107**, 6168 (2003).
- [19] R. Hinton, M. Dobrota, and T. Chard, *Density Gradient Centrifugation* (North-Holland, Amsterdam, 1978).
- [20] V. N. Manoharan, M. T. Elsesser, and D. J. Pine, *Science* **301**, 483 (2003).